Alma Mater Studiorum – Università di Bologna

DOTTORATO DI RICERCA IN

Oncologia Medica

Ciclo 35°

Settore Concorsuale: Malattie del sangue, Oncologia e Reumatologia (06/D3)

Settore Scientifico Disciplinare: Oncologia Medica (MED/06)

Understanding molecular mechanisms of resistance to immune checkpoint inhibitors in advanced non-small cell lung cancer (NSCLC)

Presentata da: Dott. Biagio Ricciuti

Coordinatore Dottorato **Supervisore**

Prof.ssa Manuela Ferracin **Prof. Andrea Ardizzoni**

Esame finale anno 2022

Abstract

Immune checkpoint inhibitors (ICI) that target PD-1/PD-L1 have recently emerged as an integral component of front-line treatment in metastatic NSCLC patients. The PD-1 inhibitor pembrolizumab is approved as monotherapy for advanced NSCLC with a PD-L1 tumor proportion score (TPS) of ≥1% and in combination with platinum doublet chemotherapy regardless of PD-L1 expression level. However, responses to either regimen occur in only a minority of cases, and PD-L1 TPS is limited as a biomarker in predicting whether a cancer will respond to PD-1 inhibition alone or would be more likely to benefit from PD-1 inhibition plus chemotherapy. Additional biomarkers of immunotherapy efficacy, such as tumor mutational burden (TMB), have not been incorporated into routine clinical practice for treatment selection. The identification of patients who have the greatest likelihood of responding to immunotherapies is critical for guiding treatment decisions. IN addition, early indicators of response could theoretically prevent patients from staying on an ineffective therapy where they might experience complications due to disease progression or develop toxicities from unnecessary exposure to an inactive agent. The aim of this research project is to investigate the clinicopathologic and molecular determinant of response/resistance to the currently available immune checkpoint inhibitors, in order to identify therapeutic vulnerabilities that can be exploited to improve the clinical outcomes of patients with advanced NSCLC.

Introduction

The initial treatment regimens for advanced non–small cell lung cancer (NSCLC) have drastically evolved over the last 15 years with the rapid development of improved genomic sequencing technologies and the emergence of immune checkpoint inhibitors. Highly active oral kinase inhibitors are now approved for several molecularly defined subsets of NSCLC, including those harboring alterations in the EGFR, ALK, ROS1, BRAF, MET, RET, and NTRK genes, although acquired resistance to these targeted therapies remains a significant clinical challenge[1]. In lung cancers lacking targetable mutations, however, programmed death 1/programmed death ligand 1 immune checkpoint inhibitors, used alone or in combination with cytotoxic T-lymphocyte-associated protein 4 inhibitors and/or cytotoxic chemotherapy, have led to meaningful improvements in overall survival. Despite the unprecedented benefit in survival with immunotherapies, only 50% respond to these treatments, and biomarkers of sensitivity and resistance to PD-(L)1 based therapies are largely unknown[2–5].

In this PhD thesis, we have dissected the clinicopathologic, genomic, and immunophenotypic correlates of immunotherapy efficacy in NSCLC with the ultimate goal of improving treatment selection for PD-(L)1 based therapies.

We had three primary aims:

1) To determine the impact of DNA damage and repair gene alterations on mutational burden and immunotherapy efficacy in NSCLC
2) To determine the differential impact of STK11 and KEAP1 mutations on PD-(L)1 inhibition resistance in KRAS mutant and KRAS wild-type NSCLC
3) To dissect the clinicopathologic, genomic and immunophenotypic correlates of tumor mutational burden in NSCLC, and its impact on immunotherapy efficacy across PD-(L)1 expression levels.

Defects in a complex network of genes that mediate the cellular response to DNA damage have been associated with improved therapeutic sensitivity to platinum chemotherapy, PARP inhibitors, and other agents across multiple

solid tumor types[6,7]. Several PARP inhibitors have recently received FDA approval in ovarian, breast, and pancreatic cancers, primarily in patients harboring BRCA mutations[8–10]. DNA repair deficiency is also an emerging biomarker of response to immune checkpoint blockade[11]. Alterations in DNA damage response and repair (DDR) genes are associated with genomic instability and increased somatic tumor mutational burden, which may enhance immunogenicity through increased tumor-specific neoantigen load[11,12]. DDR gene alterations may also enhance immune recognition and targeting via neoantigen-independent pathways, including activation of innate antitumor immunity mediated by the stimulator of interferon genes (STING) pathway[13,14]. The presence of DDR gene alterations was recently shown to be independently associated with clinical benefit to anti-PD-(L)-1 checkpoint blockade in metastatic urothelial cancer[15]. DDR gene alterations are common in NSCLC but are poorly characterized, and the clinical significance of these alterations remains unknown. In the first aim, we hypothesized that mutations in DDR genes are associated with higher tumor mutational burden (TMB) and improved clinical outcomes to PD-(L)1 inhibitor therapy in patients with advanced NSCLC.

KRAS mutations identify the largest subset of oncogene-driven lung adenocarcinoma (LUAD)[16], and co-occurring genomic alterations in STK11 and/or KEAP1 genes define a unique subset of KRAS-mutant lung cancers with distinct biology and therapeutic vulnerabilities[17]. The serine/threonine kinase 11 (STK11) gene regulates diverse cellular functions including metabolism, growth, and polarity. STK11 loss occurs in ~15% of LUAD, and is associated with a lack of PD-L1 expression, reduced tumor infiltrating cytotoxic CD8+ T lymphocytes, and resistance to ICI in patients with KRAS-mutant NSCLC[17,18]. Keap1 is a negative regulator of nuclear factor erythroid 2-related factor 2 (Nrf2), which is a master regulator of oxidative damage response 17. KEAP1 loss occurs in ~20% of NSCLC[16,19], and is associated with an immunosuppressive microenvironment characterized by low infiltration of CD8+ T cells and NK cells in mouse models[20–22]. However, data on the correlation between KEAP1 loss and outcomes to ICI in patients with advanced LUAD are conflicting, and whether this mutation impacts immunotherapy efficacy is in need of further investigation.

Because STK11 and KEAP1 mutations frequently co-occur in NSCLC, we sought to determine whether each gene mutation was independently associated with immunotherapy outcomes in NSCLC, and also to understand whether this impact was similar in both KRAS-mutant and KRAS wild-type NSCLC. To unravel the potential mechanisms by which STK11 and KEAP1 alterations affect outcomes to ICI in LUAD in this second aim of this thesis we also investigated the transcriptomic profiles of tumors harboring these mutations according to KRAS mutation status.

Tumor mutational burden (TMB), defined as the total number of non-synonymous mutations per sequenced coding area of a tumor genome, has recently emerged as a potential predictive factor of ICI efficacy across different tumor types[23]. However, in NSCLC, despite several large prospective clinical trials aimed at establishing TMB as a robust predictor of ICI therapy[24], they have not consistently demonstrated an overall survival benefit, and therefore, the role of TMB as a biomarker in NSCLC remains elusive. In the third and last primary aim of this thesis, we analyzed multiple independent cohorts of patients with NSCLC treated with PD-1/PD-L1 inhibitors to identify clinicopathologic, genomic, and immunophenotypic correlates of TMB, and to investigate TMB groupings that best discriminate responders from non-responders to ICIs, in all comers with NSCLC and in clinically relevant subgroups of PD-L1 expression.

Material and Methods

Patient population

Patients at the Dana-Farber Cancer Institute who consented to institutional review board-approved protocols DF/HCC 02-180, 11-104, 13-364, and/or 17-000 which allowed for conducting translational research and tumor next-generation sequencing, respectively, were included in in this study, and patients from Memorial Sloan Kettering Cancer Center, MD Anderson Cancer Center, Massachusetts General Hospital Stand Up to Cancer/Mark Foundation Patients were also included were enrolled (depending on the specific aim) if they had advanced NSCLC which was treated with PD-1/PD-L1 inhibitors and they had also consented to institutional review board-approved protocols.

Programmed death ligand 1 immunohistochemistry

The PD-L1 tumor proportion score (TPS) was determined by immunohistochemistry using validated anti-PD-L1 antibodies: E1L3N (Cell Signaling Technology, Danvers, MA), 22C3 (Dako North America Inc, Carpinteria, CA), 28-8 (Epitomics Inc, Burlingame, CA), according to local institutional practice.

Tumor genomic profiling and somatic variant calling and tumor mutational burden assessment

Tumor genomic profiling and somatic variants were performed using clinically validated bioinformatics pipelines. Sequence reads were aligned to reference sequence b37 edition from the Human Genome Reference Consortium using bwa (http://biobwa.sourceforge.net/bwa.shtml), and further processed using Picard (version 1.90, http://broadinstitute.github.io/picard/) to remove duplicates and Genome Analysis Toolkit (GATK) to perform localized realignment around indel sites. Single nucleotide variants were called using MuTect v1.1.4, insertions and deletions were called using GATK Indelocator, and variants were annotated using Oncotator. In the DFCI cohort, to filter out potential germline variants, the standard pipeline removed SNPs present at >0.1% in Exome Variant Server, NHLBI GO Exome Sequencing Project (ESP) (URL: http://evs.gs.washington.edu/EVS/), present in dbSNP, or present in an

in-house panel of normals, but rescues those also present in the COSMIC database. For this study, variants were further filtered by removing variants present at >0.1% in the gnomAD v.2.1.1 database or were annotated as Benign or Likely Benign in the ClinVar database[25]. In the MSKCC cohort, patient-matched normal DNA was used to filter out germline variants, as previously described[26].

DNA damage repair assessment ang gene list

For the relevent aim, DNA Damage and repair (DDR) gene assessment was perfomed using the NGS assay OncoPanel (Version 3), which surveys exonic DNA sequences of 447 cancer genes and 191 regions across 60 genes for rearrangement detection. A total of 53 were classified as DDR genes, based on literature review and expert curation including: ATM ATR BRCA1 BRCA2 BAP1 CHEK1 CHEK2 FANCA FANCB FANCC FANCD2 FANCE FANCF FANCG FANCI FANCL FANCM RAD21 RAD50 RAD51 RAD51C RAD51D RAD52 RAD54B ERCC1 ERCC2 ERCC3 ERCC4 ERCC5 ERCC6 XRCC1 XRCC2 XRCC3 XRCC4 XRCC5 XRCC6 POLB POLD1 POLE POLH POLQ NEIL1 NEIL2 NEIL3 MLH1 MLH3 MSH2 MSH6 BRIP1 PMS1 PMS2 BARD1 PALB2.

DNA damage repair gene pathway classification

For the purpose of this the relevant aim examining the impact of DDR mutations on clinical outcomes to immunotherapies, the individual 53 DNA damage repair genes were classified in the following functional pathways:

- Mismatch Repair: MLH1, MLH3, MSH2, MSH6, PMS1, PMS2
- DNA Damage Sensing: ATM, ATR, CHEK1, CHEK2
- Homologous Recombination: BRCA1, BRCA2, RAD50, RAD51, RAD51C, RAD51D, RAD52, RAD54B, PALB2, BRIP1, BARD1, BAP1
- Nucleotide Excision Repair: ERCC1, ERCC2, ERCC3, ERCC4, ERCC5, ERCC6
- Base excision Repair: XRCC1, XRCC2, XRCC3, XRCC4, XRCC5, XRCC6
- DNA Polymerase: POLB, POLD1, POLE, POLH, POLQ

- Fanconi Anemia: FANCA, FANCB, FANCC, FANCD2, FANCE, FANCF, FANCG, FANCI, FANCL, FANCM.

Determination of DDR genes deleterious mutation status

For the aim of this thesis relative to the impact of DDR mutations on immunotherapy efficacy, all loss-of-function mutations in DDR genes (including nonsense, frameshift, or splice site) were classified as deleterious. To determine the pathogenicity of missense mutations we used a three-step approach. First, we reviewed all the identified missense mutations in the Catalogue of Somatic Mutations in Cancer (COSMIC) and ClinVar databases. Second, we performed an in silico functional analysis using the PolyPhen-2 (Polymorphism Phenotyping v2) prediction tool²⁷²⁷²⁷²⁷²⁷²⁷²⁷²⁷²⁷²⁷²⁷²⁷²⁷ to determine the functional significance of each missense mutation[28]. Third, because only tumor tissue was sequenced, common single nucleotide polymorphisms (SNPs) were filtered if present at >0.1% frequency in Genome Aggregation Database (gnomAD) version 2.1.1 (http://gnomad.broadinstitute.org/ last accessed May 15th, 2019). Missense mutations reported as pathogenic by COSMIC and/or ClinVar or with a PolyPhen-2 score of ≥0.95 (“probably damaging”), were classified as deleterious. Patients harboring any deleterious DDR mutations were defined as DDR positive, while patients without deleterious DDR mutations were defined as DDR negative.

Determination of STK11 and KEAP1 mutation status

LUADs were characterized as STK11- or KEAP1-mutant if they harbored loss-of-function alterations, including nonsense, frameshift, insertion/deletion, or splice site mutations in these genes. To determine the pathogenicity of missense mutations, we employed a two-step approach. First, we reviewed all the identified missense mutations in the Catalogue of Somatic Mutations in Cancer (COSMIC). Second, we performed an in silico functional analysis using the PolyPhen-2 (Polymorphism Phenotyping v2) prediction tool to determine the functional significance of each missense mutation5. Only missense

mutations reported as pathogenic by COSMIC and/or probably damaging by PolyPhen-2 were classified as deleterious. KEAP1 mutation status was not available for the MDACC cohort.

Tumor mutational burden assessment

Tumor mutational burden (TMB), defined as the number of somatic, coding, base substitution, and indel mutations per megabase (Mb) of genome examined, was determined using the OncoPanel (Dana-Faber)[25] and MSK-IMPACT (MSKCC)[26] NGS platforms for the relevant aims, as previously described. DFCI mutation counts were divided by the number of bases covered in each OncoPanel version: v1, 0.753334 Mb; v2, 0.826167 Mb; and v3, 1.315078 Mb. For MSKCC samples, the mutation count was divided by 0.896665, 1.016478, and 1.139322 Mb for the 341-, 410-, and 468-gene panels, respectively. From NSCLC samples which underwent whole exome sequencing (SU2C/Mark Foundation Cohort) DNA was extracted from FFPE tumor specimens and either matched normal whole blood or in cases where this was unavailable, adjacent normal FFPE specimens. Extraction was performed using the Qiagen AllPrep DNA/RNA Mini Kit (cat#80204). A single aliquot of 150-500 ng input DNA in 100 µl TE buffer was used for library generation. Library preparation was performed using the Kapa HyperPrep kit, and quantification was performed using PicoGreen. Adapter ligation was performed using the TruSeq DNA exome kit from Illumina per manufacturer's instructions. Sequencing of pooled libraries was performed using a HiSeq2500 with 76 bp paired end reads. Mean target coverage for tumor and normal samples were 150X and 80X, respectively. Tumor mutational burden was defined as the number of non-synonymous base substitutions, indel mutations per megabase of genome examined, using an exome size of 35.8 Mb.

Tumor mutational burden normalization across different platformsTMB distributions were harmonized between different platforms by applying a normal transformation followed by standardization to Z-scores. Power transformations were first used to normalize cohort-specific TMB distributions; second, Tukey's ladder of powers in the rcompanion package was used to identify the optimal transformation coefficient. Third, the normalized distributions were then

standardized into z scores by subtracting the transformed distribution mean and dividing by the standard deviation.

Cell subset analysis from the TCGA dataset

To perform cell type enrichment analyses for the respetive aims of this thesis, RNA sequencing data from the LUAD and LUSC TCGA cohort were deconvoluted to estimate cell subsets using the xCell package[29]. xCell estimates the abundance scores of 64 cell types, including adaptive and innate immune cells, hematopoietic progenitors, epithelial cells, and extracellular matrix cells, based on single sample gene set enrichment analysis (ssGSEA) data. Gene expression values (RSEM V2) were converted into Z-scores and used to compute cell type enrichment scores with the xCellAnalysis function. Statistical significance of differential cell type enrichment between cohorts was estimated with Wilcox Rank Sum test. Cell subtypes examined included: aDC, Adipocytes, Astrocytes, B-cells, Basophils, CD4+ memory T-cells, CD4+ naive T-cells, CD4+ T-cells, CD4+ Tcm, CD4+ Tem, CD8+ naive T-cells, CD8+ T-cells, CD8+ Tcm, CD8+ Tem, cDC, Chondrocytes, Class-switched memory B-cells, CLP, CMP, DC, Endothelial cells, Eosinophils, Epithelial cells, Erythrocytes, Fibroblasts, GMP, Hepatocytes, HSC, iDC, Keratinocytes, Endothelial cells, Macrophages, Macrophages M1, Macrophages M2, Mast cells, Megakaryocytes, Melanocytes, Memory Bcells, MEP, Mesangial cells, Monocytes, MPP, MSC, Endothelial cells, Myocytes, naive B-cells, Neurons, Neutrophils, NK cells, NKT, Osteoblast, pDC, Pericytes, Plasma cells, Platelets, Preadipocytes, pro B-cells, Sebocytes, Skeletal muscle, Smooth muscle, Tgd cells, Th1 cells, Th2 cells, Tregs.

Gene expression analysis

Gene expression data were downloaded from the Firehose website (TCGA Firehose Legacy version) while somatic mutation data were downloaded from cBioPortal website (cbioportal.org). The RSEM V2 values were used to represent gene expression and genes with counts less than 10 were filtered out. Gene expression profiles were analyzed according to TMB categories. Median expression within each group was used to estimate expression fold-change (FC) to minimize the possible impact of outlier samples. Gene

differential expression analyses across TMB subgroups were conducted using R package DESeq2. Pvalues were corrected for multiple hypothesis testing via false discovery rate (FDR) adjustment. Fold-change threshold of an absolute value greater than 1.5 and FDR adjusted P-value threshold less than 0.1 were utilized to identify differentially expressed genes. Pathway enrichment analyses were conducted separately for up- and down-regulated genes using Molecular Signatures Database (MSigDB) collections.

Statistical analysis

Clinicopathologic data and immunotherapy response data were abstracted from the electronic medical record. Overall response rate was determined by a blinded radiologist using Response Evaluation Criteria In Solid Tumors, version (RECIST) 1.1. Progression-free survival was determined from the start date of immunotherapy until the date of disease progression or death, and overall survival was calculated from the date of diagnosis of advanced NSCLC until the date of death. All p-values are twosided and confidence intervals are at the 95% level. Overall survival among patients who never received PD-(L)1 inhibition was calculated from the date of the start of systemic therapy for advanced disease, other than immunotherapy. TMB comparisons were computed using the Mann-Whitney U test or the Kruskal-Wallis test, when appropriate. Linear correlations were evaluated using Spearman's test, and categorical variables were evaluated using Fisher's exact test. Event-time distributions were estimated using Kaplan-Meier methodology. Log-rank tests were used to test for differences in event-time distributions, and Cox proportional hazards models were fitted to obtain estimates of hazard ratios in univariate and multivariate models. The proportional hazards assumption was assessed with Schoenfeld residuals. All P-values are 2-sided and confidence intervals are at
the 95% level, with significance pre-defined to be at <0.05. Multiple comparison correction was performed using the BenjaminiHochberg procedure. Missing values were handled using inverse probability weighting (IPW) and multiple imputation approaches using R package MICE, as previously described. All statistical analyses were performed using R version 3.6.3.

For the relative aim, To identify and validate TMB thresholds associated with immunotherapy efficacy, an unbiased recursive partitioning algorithm was used

to investigate an optimal grouping of TMB with respect to the objective response rate to immune checkpoint inhibition in a discovery cohort comprised of patients from the MSKCC cohort, using the partykit function in R, as previously described. A 10-fold cross-validation method was used to train and measure the performance of the model using the caret function in R, as previously described. The threshold identified was validated in two independent cohorts of patients treated with PD-(L)1 blockade in the DFCI and SU2C/Mark Foundation cohorts, following TMB harmonization across platforms, as described above and as previously described. As PD-L1 tumor proportion score (TPS) is an important predictor for ICI efficacy, we applied both Inverse probability weighting (IPW) and multiple imputation approaches using R package MICE to address the potential selection bias arising from the PD-L1 TPS missingness. Variables used for multiple imputation and to calculate the weights for PD-L1 TPS missingness included sex, age, ECOG performance status, histology, smoking status, and line of therapy for ICI. IPW and multiple imputation were conducted separately in each cohort, and the multivariable analyses results were pooled based on 5 repeated complete imputed datasets.

Results

Aim#1 To determine the impact of DNA damage and repair gene alterations on mutational burden and immunotherapy efficacy in NSCLC

A total of 266 patients with advanced NSCLC and successful tumor NGS who were treated with PD-(L)1 inhibitor therapy at the Dana-Farber Cancer Institute (DFCI) between January 2014 and September 2018 were identified. The median age of the cohort was 66 years (range: 35-92), most patients had a history of tobacco use (83.5%), and the majority of tumors demonstrated adenocarcinoma histology (80.8%). In the entire cohort, an activating *KRAS* mutation was found in 33.4% of cases, while an *EGFR* activating mutation was identified in 10.2% of cases. The median PD-L1 expression was 50% (interquartile range: 2.75-90), while the median TMB was 9.18 mutations/Megabase (mut/Mb) (range: 0.76-54.75). Tumors from 132 patients

(49.6%) were defined as DDR-positive, while the remaining 134 (50.4%) were defined as DDR-negative (**Figure 1**).

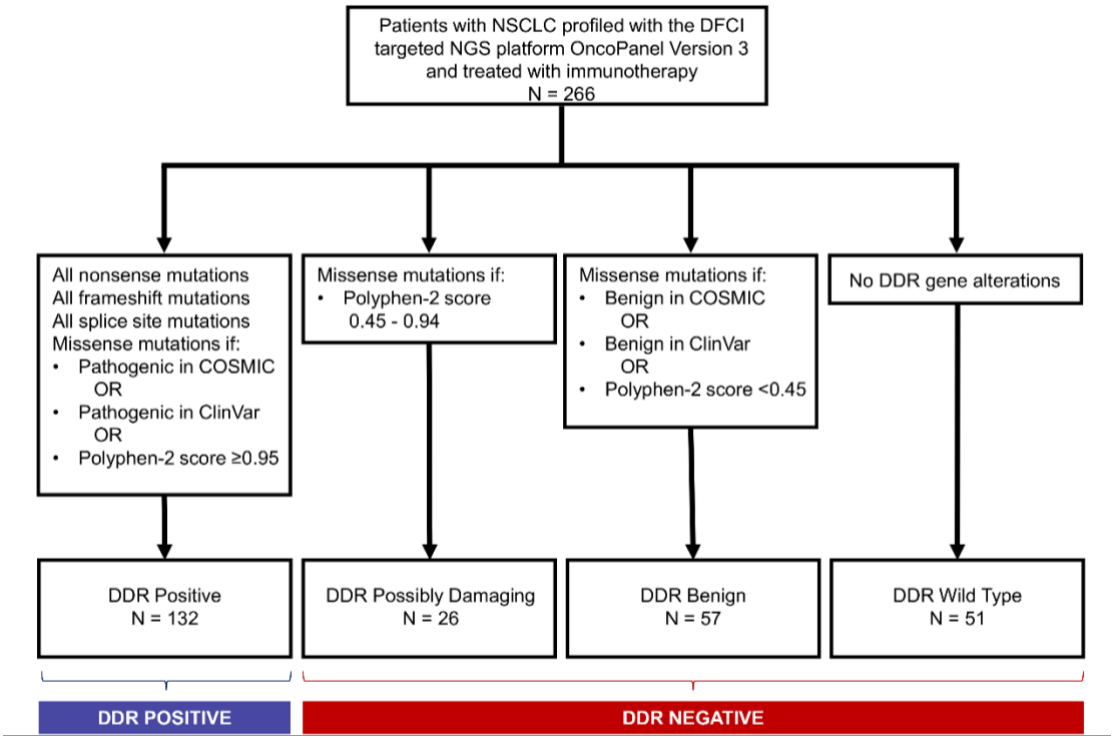

Figure 1. Study flow chart of the 266 patients included in this study. One hundred thirty-two NSCLCs (49.6%) were defined as DDR-positive, while the remaining 134 (50.4%) were defined as DDR-negative. DDR, DNA damage response and repair.

Of these, 143/201 (71.1%) consisted of missense mutations while the remaining included nonsense, splice site, and frameshift alterations. Among DDR-positive NSCLCs, the most commonly mutated DDR genes were *ATM* (9.4%), *ATR* (4.8%), *BRCA2* (4.1%), *POLQ* (3.7%), and *RAD50* (3.0%). Fifteen tumors (11.3%) with deleterious DDR mutations in *RAD50* (n = 2), *BRCA2* (n = 2), *ATM*, *ATR*, *MLH3*, *NEIL1*, *BAP1*, *CHEK2*, *ERCC5*, *POLQ*, *RAD21*, *RAD51D*, *XRCC4* (n = 1 each) also demonstrated concomitant copy loss in the respective gene, consistent with loss of heterozygosity. The baseline clinical and pathological characteristics of the DDR-positive and DDR-negative groups were well balanced in terms of age, sex, performance status, histology, presence of brain metastasis prior to PD-(L)1 inhibitor treatment start, line of therapy, and PD-L1 expression level (**Table 1**).

Clinical Characteristic	DDR positive N = 132 (%)	DDR negative N = 134 (%)	P value
Age, median (range)	66 (35-92)	67 (35-90)	0.31
Sex			
Male	58 (43.9)	61 (45.5)	0.81
Female	74 (56.1)	73 (54.5)	
Smoking status			
Current/Former	110 (83.3)	112 (83.6)	1.0
Never	22 (16.7)	22 (16.4)	
Histology			
Adenocarcinoma	106 (80.3)	109 (81.3)	
Squamous cell carcinoma	19 (14.4)	15 (11.2)	0.59
NSCLC NOS	7 (5.3)	10 (7.5)	
Oncogenic driver mutation			
KRAS	45 (34.1)	44 (32.8)	
EGFR	9 (6.8)	18 (13.4)	0.35
Other	22 (16.7)	20 (14.9)	
None identified	56 (42.4)	52 (38.8)	
Concurrent TP53 mutation			
Yes	78 (59.1)	86 (64.1)	0.45
No	54 (18.1)	48 (35.9)	
Concurrent STK11 mutation			
Yes	20 (15.2)	20 (14.9)	0.99
No	112 (84.8)	114 (85.1)	
ECOG performance status			
0-1	105 (79.5)	100 (76.6)	0.38
≥2	27 (20.5)	34 (25.4)	
Brain metastases prior to immunotherapy			0.69
Yes	42 (31.8)	39 (29.1)	
No	90 (68.2)	95 (70.9)	
Line of therapy			
1st	64 (48.5)	52 (38.8)	0.14
≥2nd	68 (51.5)	82 (61.2)	
PD-L1 expression			
<1%	12 (10.1)	22 (17.9)	
1-49%	41 (34.5)	37 (30.1)	0.21
≥50%	66 (55.5)	64 (52.0)	
Not assessed	13	11	

Table 1: Characteristics of patients with NSCLC by DDR mutation status

The median TMB was significantly higher in the DDR-positive group compared to the DDR-negative group (12.1 versus 7.6 mut/Mb, P<0.001) (**Figure 2A**). Most patients had deleterious mutations in only one DDR gene (85/132, 64.4%), while 35.6% (47/132) of patients had mutations in ≥2 DDR genes. The median TMB was significantly higher among patients with ≥2 DDR gene mutations compared to those with one DDR gene mutation or with a DDR-negative genotype (15.2 versus 10.6 versus 7.6 mut/Mb, P<0.001, **Figure 2B**).

Among smokers, DDR-positive cases had a significantly higher median TMB compared to DDR-negative cases (12.9 versus 8.3 mut/Mb, P<0.001, **Figure 2C**). Similarly, among never smokers, DDR-positive cases had also a significantly higher median TMB compared to DDR-negative cases (8.7 versus 5.7 mut/Mb, P=0.04, **Figure 2C**).

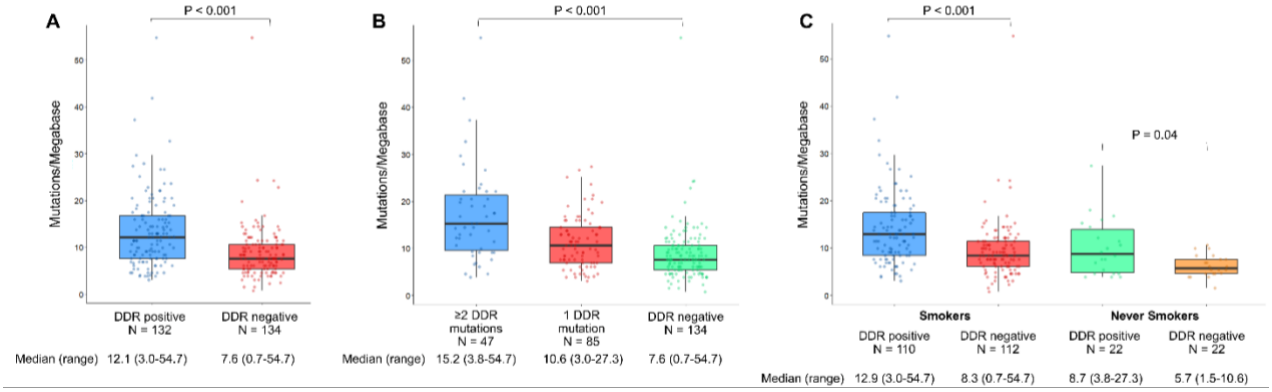

Figure 2. (A) Tumor mutational burden (TMB) by DDR gene mutation status. (B) Tumor mutational burden by the number of DDR gene alterations. (C) Tumor mutational burden by DDR mutation among smokers and never smokers. DDR, DNA damage response and repair.

We next examined the clinical outcomes to PD-(L)1 inhibition according to DDR mutation status. In the DDR-positive group, the ORR was 30.3% (95%CI: 22.6-38.9), which was significantly higher compared to the ORR of 17.2% (95%CI: 11.2-24.6) observed in the DDR-negative group (P = 0.01, **Figure 3A**). The median PFS (mPFS) was significantly longer in the DDR-positive group compared to the DDR-negative group (5.4 versus 2.2 months, HR: 0.58 [95%CI: 0.45-0.76], P<0.001, **Figure 3B**). The median OS (mOS) was also significantly longer in the DDR-positive group compared to the DDR-negative group (18.8 versus 9.9 months, HR: 0.57 [95%CI: 0.42-0.77], P<0.001, **Figure 3C**). As multicollinearity was not detected between PD-L1, TMB, DDR mutation

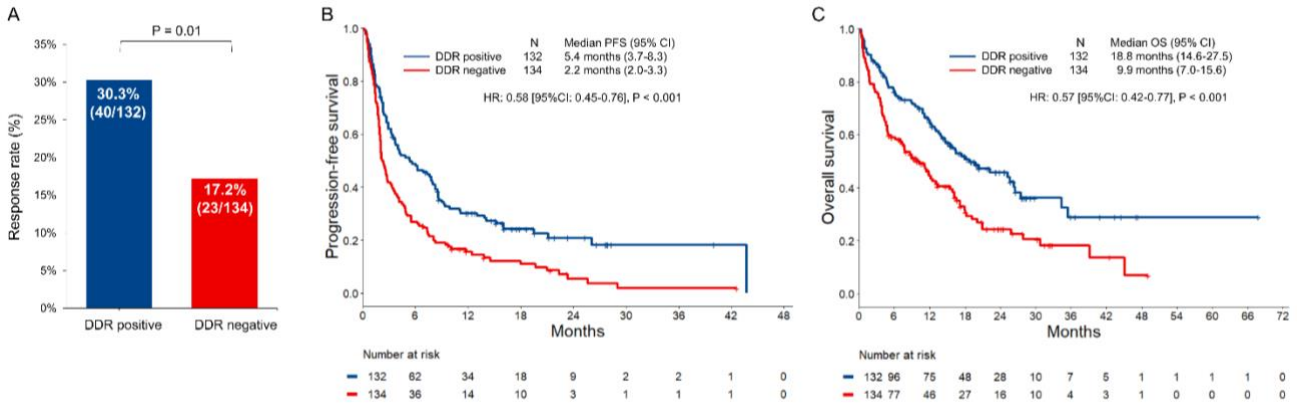

Figure 3. (A) Response rate, (B) progression-free and (C) overall survival in patients treated with PD-(L)1 inhibitor therapy in the DDR-positive and DDR-negative groups**.**

As first-line pembrolizumab represents a first-line treatment option for patients with NSCLC and a PD-L1 expression level of ≥50%, we also investigated the impact of DDR mutation status in this specific clinical context. In the entire cohort of 266 patients, 92 (34.6%) had NSCLC with a PD-L1 expression level of ≥50% and received first-line pembrolizumab monotherapy. In this group, 49 (53.3%) cases were DDR-positive and 43 (46.7%) were DDR-negative. Baseline clinical and pathological features were well balanced between the two cohorts with the only exception of median TMB, which was significantly higher in the DDR-positive group compared to the DDR-negative group (13.7 versus 7.6 mut/Mb, P<0.001). The ORR was significantly higher in the DDR-positive group compared to the DDR-negative group (53.1% [95%CI: 38.2-67.5] versus 25.6% [95%CI: 13.5-41.2], P=0.01, **Figure 4A**). The mPFS was significantly longer in the DDR-positive group compared to the DDR-negative group (13.0 versus 3.1 months, HR: 0.35 [95%CI: [0.21-0.60], P<0.001, **Figure 4B**). The mOS was also significantly longer in the DDR-positive group compared to the DDR-negative group (not reached [NR] versus 13.3 months, HR: 0.37 [95%CI: 0.20-0.70], P<0.01, **Figure 4C**). After adjusting for TMB and performance status, the presence of a deleterious DDR gene mutation was associated with significantly longer PFS (HR: 0.43 [95%CI: 0.24-0.78], P=0.01) and OS (HR: 0.42 [95%CI: 0.21-0.86], P=0.02) in multivariate analysis also among patients with a PD-L1 expression of ≥50% treated with first-line pembrolizumab monotherapy analysis.

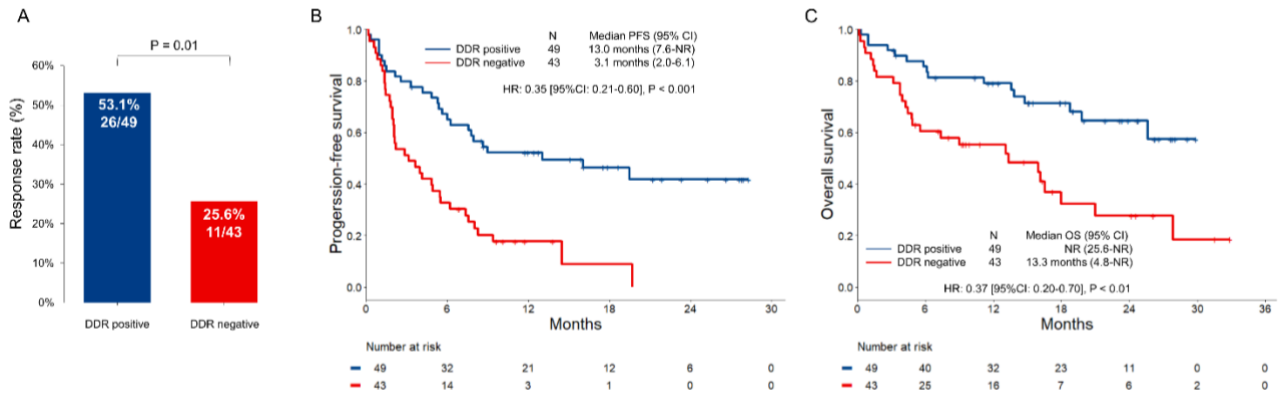

Figure 4. (A) Response rate, (B) progression-free and (C) overall survival in patients with PD-L1 expression ≥50% treated with first-line pembrolizumab monotherapy in DDR-positive and DDR-negative NSCLC.

Aim#1 To determine the differential impact of STK11 and KEAP1 mutations on PD-(L)1 inhibition resistance in KRAS mutant and KRAS wild-type NSCLC.

We identified a total of 1261 patients with advanced LUAD who received PD-(L)1 inhibition, with 620 (49.2%) in a discovery cohort comprised of cases from the DFCI/MGH cohort and 641 (50.8%) in a validation cohort from the MSKCC/MDACC cohort. In the combined cohort, co-occurring mutations in *KRAS/STK11*, *KRAS/KEAP1,* and *STK11/KEAP1* were found in 10.9% (138/1261), 8.4% (101/1202), and 9.4% (113/1202) of *KEAP1* evaluable cases, respectively (**Figure 5**).

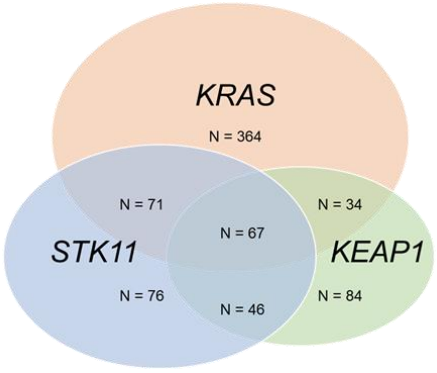

Figure 5. Venn diagram showing the overlap between *KRAS*, *STK11*, and *KEAP1* mutations.

We first analyzed the impact of *KRAS*, *STK11*, and *KEAP1* mutation status on PD-L1 expression and TMB by KRAS mutation status. When analyzed by *KRAS* status, *STK11* alterations were associated with significantly lower PD-L1 expression among both *KRAS*^{MUT} and *KRAS*^{WT} LUADs, while *KEAP1* mutations was associated with lower PD-L1 expression predominantly among *KRAS*^{MUT} but not *KRAS*^{WT} cases (**Figure 6A-B**). When TMB distributions were analyzed according to *KRAS* status, LUADs harboring *STK11* mutations had a higher TMB only among *KRAS*^{MUT} but not *KRAS*^{WT} cancers in the MSKCC/MDACC and in the combined cohort, while *KEAP1*^{MUT} tumors had consistently higher TMB only among *KRAS*^{MUT} but not *KRAS*^{WT} cases, in all the cohorts examined (**Figure 6C-D**).

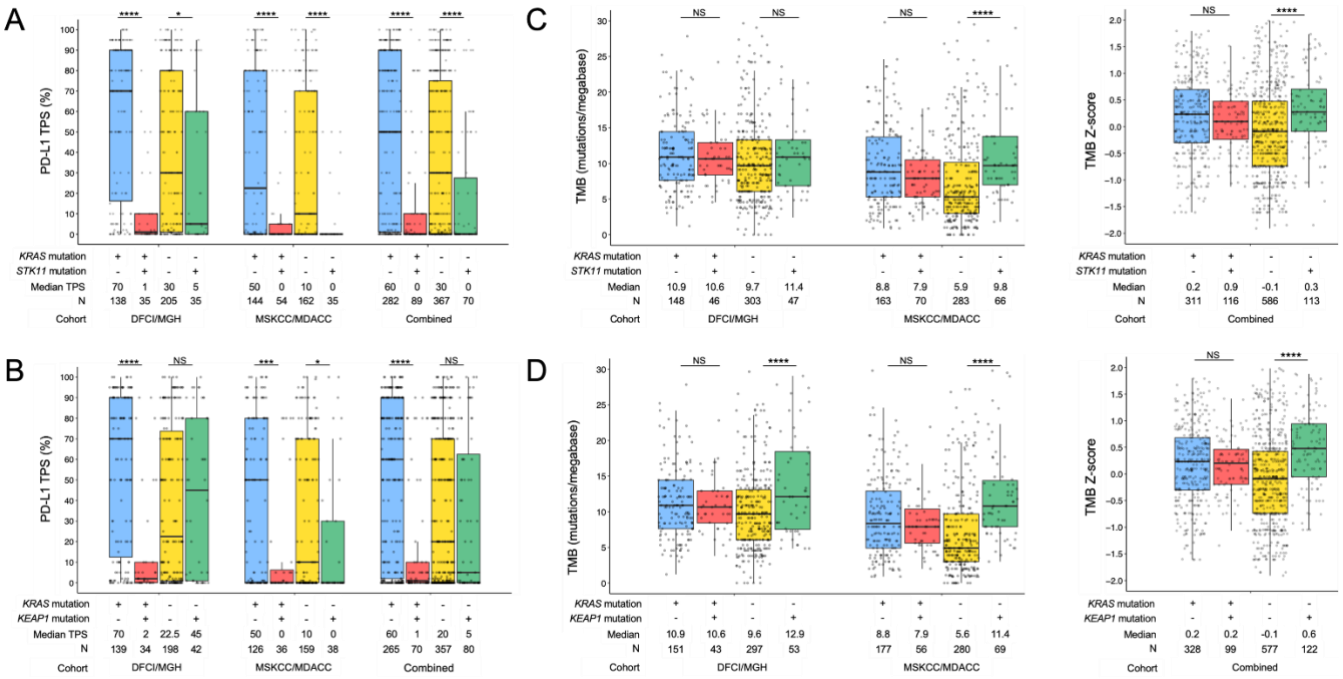

Figure 6. PD-L1 expression according to (A) KRAS/STK11 co-mutation status and (B) KRAS/KEAP1 co-mutation status, in the DFCI/MGH, MSKCC/MDACC, and combined cohorts. (C) Tumor mutational burden according to KRAS/STK11 co-mutation status, in the DFCI, MSKCC/MDACC and combined cohorts. (D) Tumor mutational burden according to KRAS/KEAP1 co-mutation status, in the DFCI/MGH, MSKCC/MDACC and combined cohorts. TPS, tumor proportion score. TMB, tumor mutational burden. NS, not significant; *, P<0.05; **, P<0.01; ***, P<0.001; ****, P<0.0001.

We next analyzed the impact of *STK11* and *KEAP1* mutation on ICI efficacy in the context of *KRAS* mutation status. Both STK11 and KEAP1 mutations were associated with worse response rate to PD-(L)1 blockade in KRAS mutant but not KRAS wild type NSCLC (**Figure 7**).

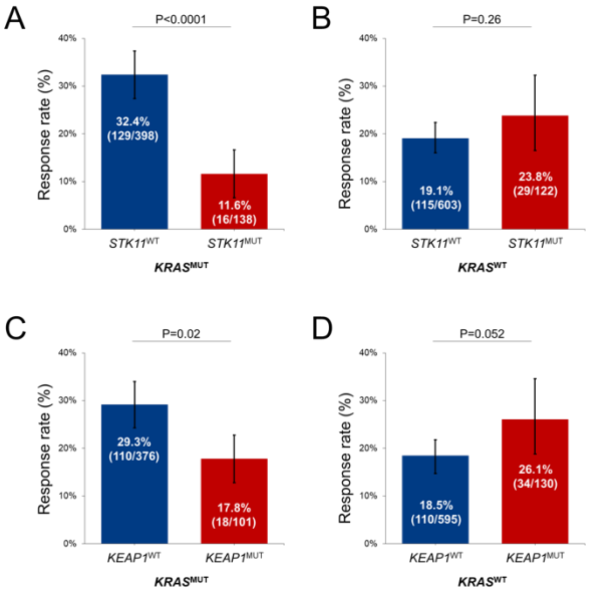

Figure 7. Objective response rate to PD-(L)1 inhibition according to STK11 mutation status among (A) KRAS MUT and (B) KRAS WT LUADs in the combined cohort. Objective response rate to PD-(L)1 inhibition according to KEAP1 mutation status among (C) KRAS MUT and (D) KRAS WT LUADs in the combined cohort.

Consistently, we noted significantly worse progression-free survival and overall survival with PD-(L)1 blockade in KRAS mutant NSCLC, but not KRAS wild type NSCLC, with loss of function mutations in STK11 (**Figure 8**), and KEAP1 (**Figure 9**).

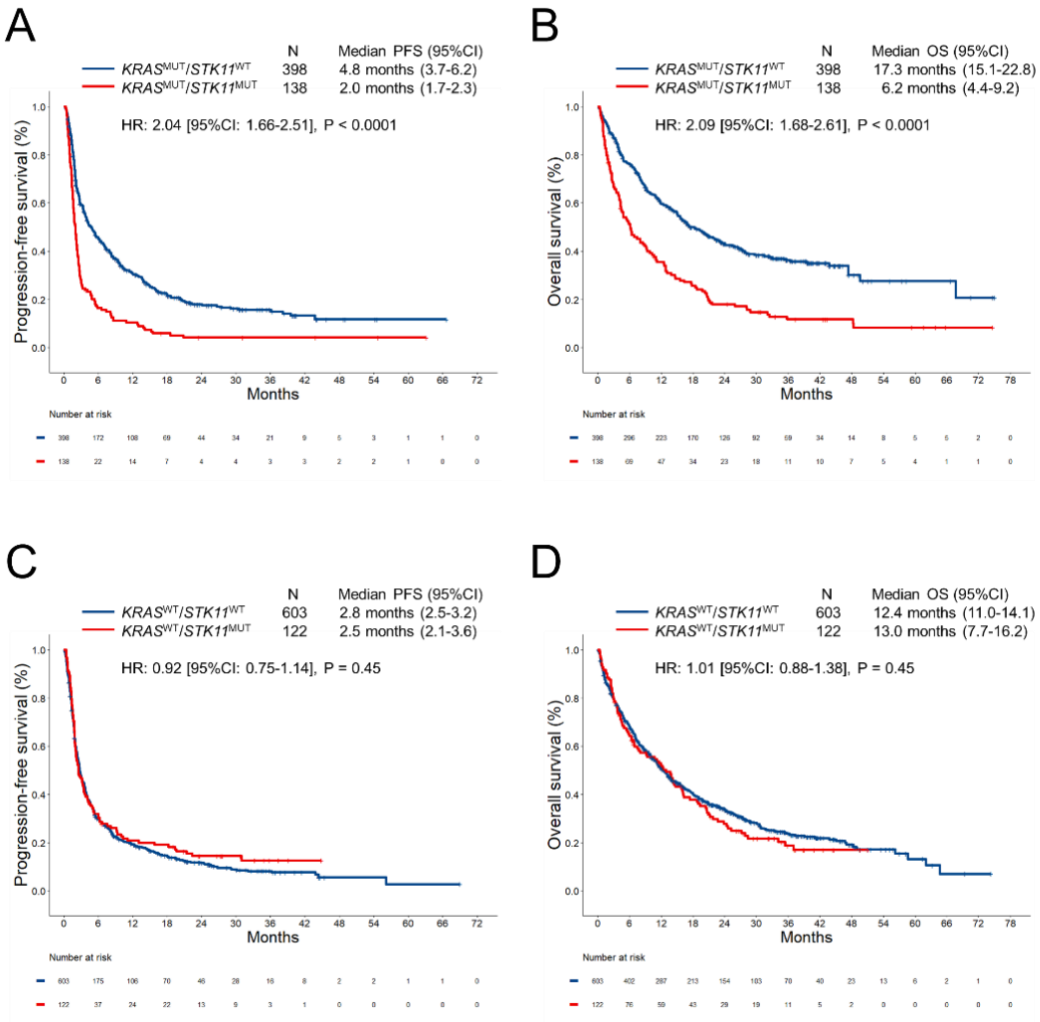

Figure 8. (A) Progression-free, and (B) overall survival to PD-(L)1 inhibition according to STK11 mutation status among KRASMUT LUADs in the combined cohort (DFCI/MGH + MSKCC/MDACC). (C) Progression-free, and (D) overall survival to PD-(L)1 inhibition according to STK11 mutation status among KRASWT LUADs in the combined cohort (DFCI/MGH + MSKCC/MDACC).

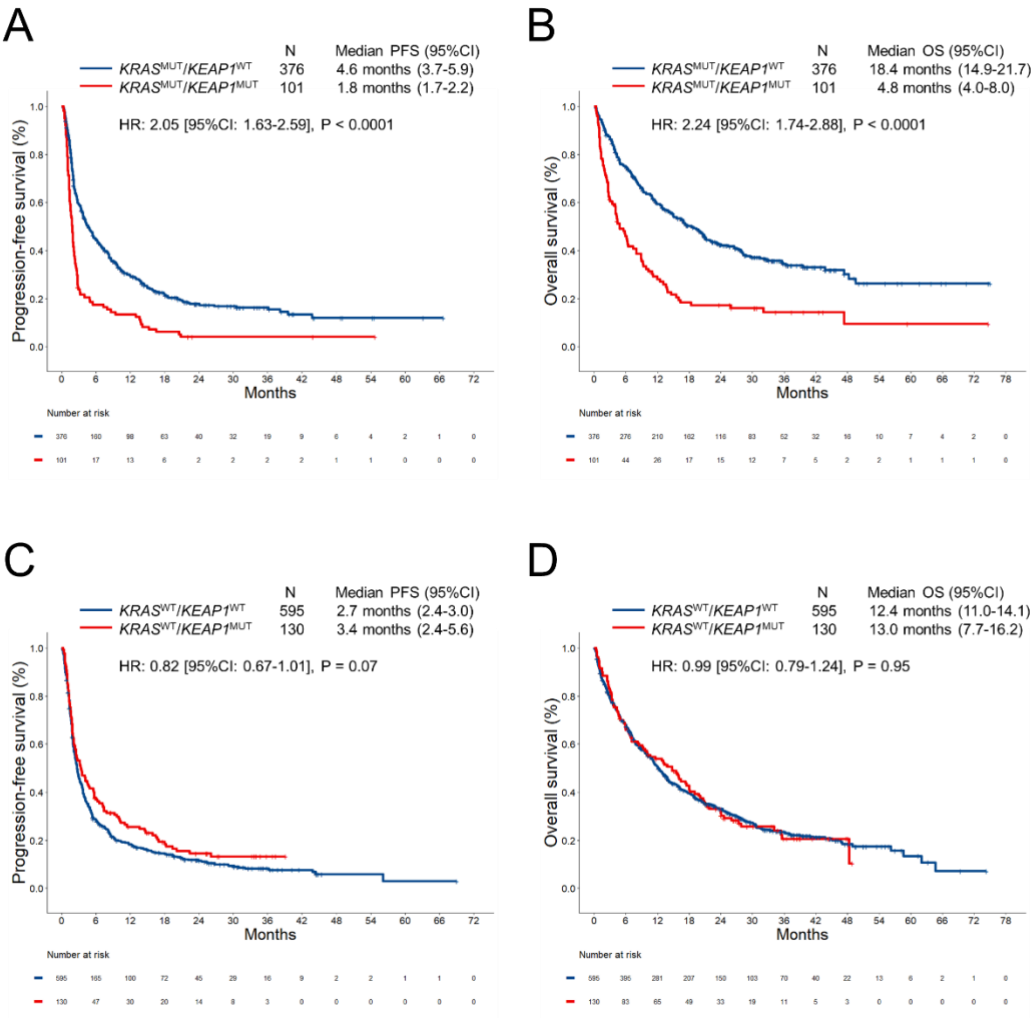

Figure 9. (A) Progression-free, and (B) overall survival to PD-(L)1 inhibition according to KEAP1 mutation status among KRAS MUT LUADs in the combined cohort (DFCI/MGH + MSKCC/MDACC). (C) Progression-free, and (D) overall survival to PD-(L)1 inhibition according to KEAP1 mutation status among KRAS WT LUADs in the combined cohort (DFCI/MGH + MSKCC/MDACC).

To unravel the potential mechanisms by which the deleterious impact of *STK11* and *KEAP1* mutations on outcomes to ICI in LUAD is primarily driven by *KRAS* mutation, we investigated the transcriptomic profiles of tumors harboring these mutations in *KRAS*^{MUT} and *KRAS*^{WT} LUADs. RNA sequencing data of 513 LUADs in the TCGA dataset were analyzed according to *KRAS/STK11* and *KRAS/KEAP1* co-mutation status. We first identified genes that were differentially expressed among *KRAS*^{MUT}/*STK11*^{WT} vs *KRAS*^{MUT}/*STK11*^{MUT} LUADs and among *KRAS*^{WT}/*STK11*^{WT} vs *KRAS*^{WT}/*STK11*^{MUT} cancers. Next, we performed a hierarchical gene ontology analysis only on the subsets of genes which were differentially regulated in *KRAS*^{MUT}/*STK11*^{WT} tumors vs

KRAS^{MUT}/*STK11*^{MUT} but not among *KRAS*^{WT}/*STK11*^{WT} vs *KRAS*^{WT}/*STK11*^{MUT}. Among the 22 significant terminal pathways identified thirteen involved in immune-mediated processes were markedly downregulated in *KRAS*^{MUT}/*STK11*^{MUT} compared to *KRAS*^{MUT}/*STK11*^{WT} LUADs, including the MHC class II protein complex, T-cell activation, immune response activating signaling, leukocyte migration, leukocyte degranulation, and myeloid leukocyte activation, among others (**Figure 10A**). We next identified genes that were differentially expressed among *KRAS*^{MUT}/*KEAP1*^{MUT} versus *KRAS*^{MUT}/*KEAP1*^{WT} LUADs and among *KRAS*^{WT}/*KEAP1*^{MUT} vs *KRAS*^{WT}/*KEAP1*^{WT} cancers and performed gene ontology analysis on the subsets of genes which were uniquely upregulated in *KRAS*^{MUT}/*KEAP1*^{WT} tumors vs *KRAS*^{MUT}/*KEAP1*^{MUT}. Among the 13 terminal pathways identified, 11 were involved in immune-related processes, including the following gene ontology terms: external side of plasma membrane, regulation of T-cell activation, T-cell receptor signaling, defense response to virus, regulation of leukocyte cell-to-cell adhesion, and lymphocyte migration (**Figure 10B**).

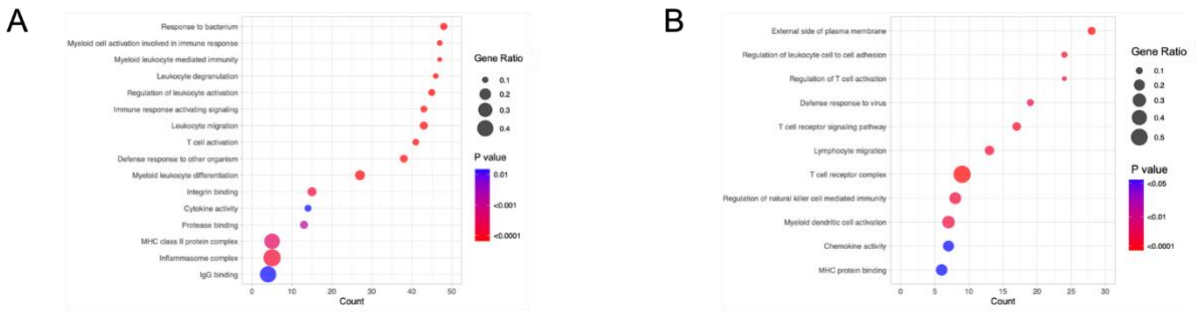

Figure 10. (A) Bubble plot showing the 13 prioritized immune-related pathways which are significantly downregulated in KRAS MUT/STK11 MUT compared to KRAS MUT/STK11 WT LUADs, but not in KRAS WT/STK11 MUT compared to KRAS WT/STK11 WT LUADs. (B) Bubble plot showing the 11 prioritized immune-related pathways which are significantly downregulated in KRASMUT/KEAP1MUT compared to KRASMUT/KEAP1WT LUADs, but not in KRAS WT/KEAP1 MUT compared to KRAS WT/KEAP1 WT LUADs.

Aim #3. To dissect the clinicopathologic, genomic and immunophenotypic correlates of tumor mutational burden in NSCLC, and its impact on immunotherapy efficacy across PD-(L)1 expression levels.

A total of 3591 NSCLC samples at DFCI which underwent tumor genomic profiling were used to identify clinical, histologic, and genomic characteristics associated with TMB. The median age was 66 years (range:18-99) and 78.3% of patients had a history of tobacco use. The median TMB was 9.8 mutations/megabase (mut/Mb) (range: 0-104.9, **Figure 11A**). TMB values were highest among current smokers, followed by former smokers, and lowest among never smokers (**Figure 11B**); there was a linear correlation between TMB and pack-years of tobacco use (**Figure 11C**). TMB distributions were comparable in squamous and nonsquamous histologies among tobacco-

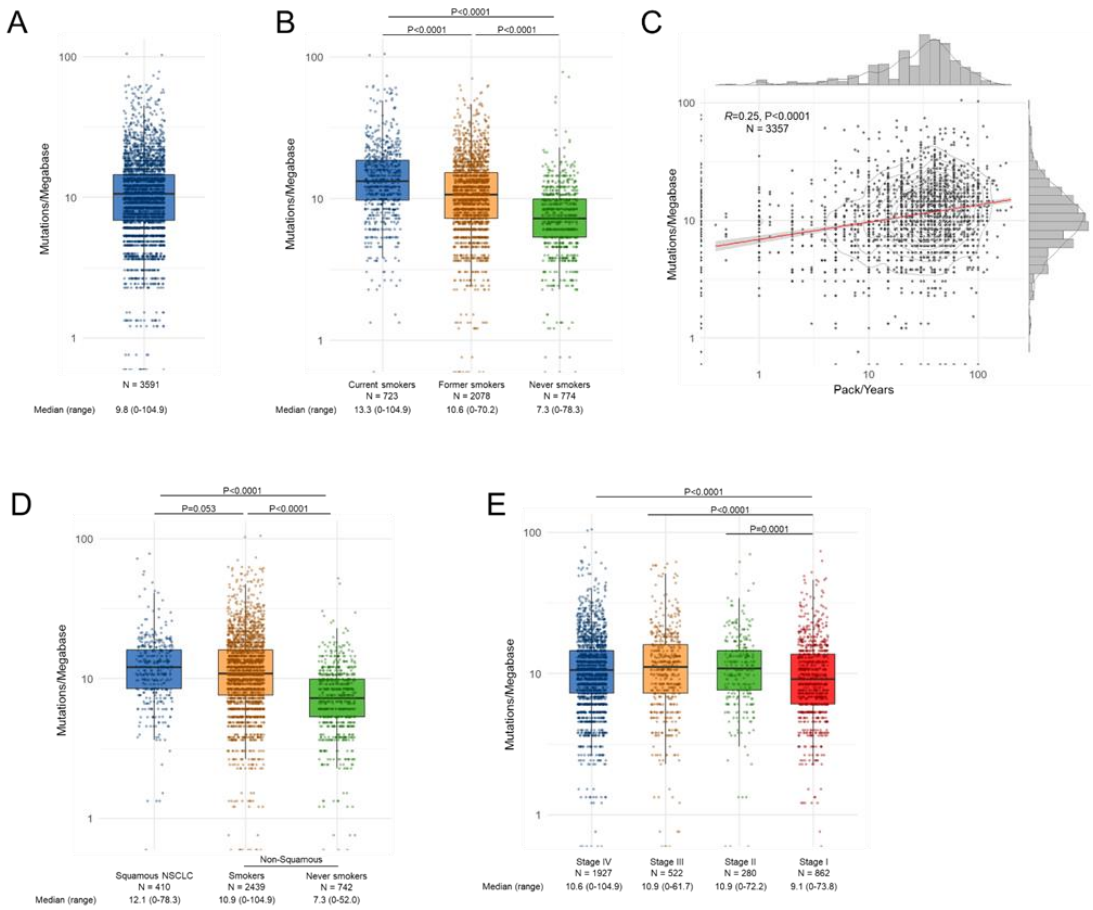

Figure 11. (A) Tumor mutational burden of 3591 NSCLCs which underwent next-generation sequencing at the Dana-Farber Cancer Institute. Correlation between TMB with (B) tobacco history, (C) number of tobacco pack-years, (D) tumor histology, (E) NSCLC stage at the time of next generation sequencing.

associated NSCLCs (**Figure 11D**). TMB was higher in stage II, III, and IV

NSCLCs compared with stage I NSCLCs (**Figure 11E**). When analyzed by oncogenic mutation status, NSCLCs with activating mutations in *BRAF* and *KRAS* had the highest TMB, as did those without an identifiable driver mutation, while NSCLCs driven by *EGFR* mutations and chromosomal rearrangements in *RET* and *ALK* had the lowest TMB of the cases examined (**Figure 12**).

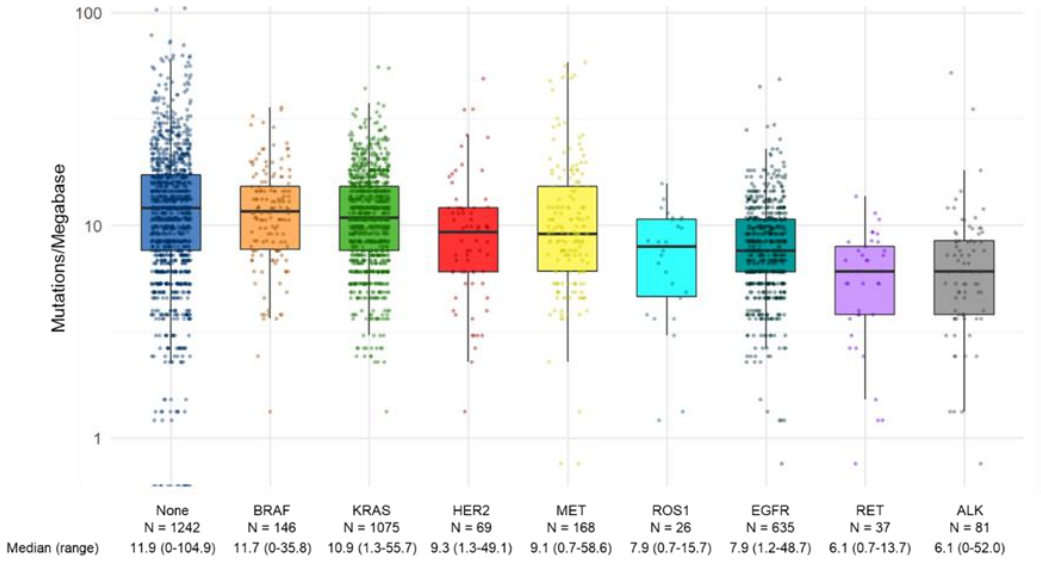

Figure 12. (A TMB distributions according to NSCLC genotype

We next investigated the impact of TMB on clinical outcomes among patients who received ICI at MSKCC (N = 672), DFCI (N = 714), and SU2C (N = 166). Because TMB was estimated with different platforms in the MSKCC (MSK-IMPACT), DFCI (DFCI OncoPanel) and in the SU2C/Mark Foundation cohorts (whole exome sequencing), we first harmonized the TMB distribution across the three platforms, by applying a normal transformation followed by standardization to Z-scores (**Figure 13**).

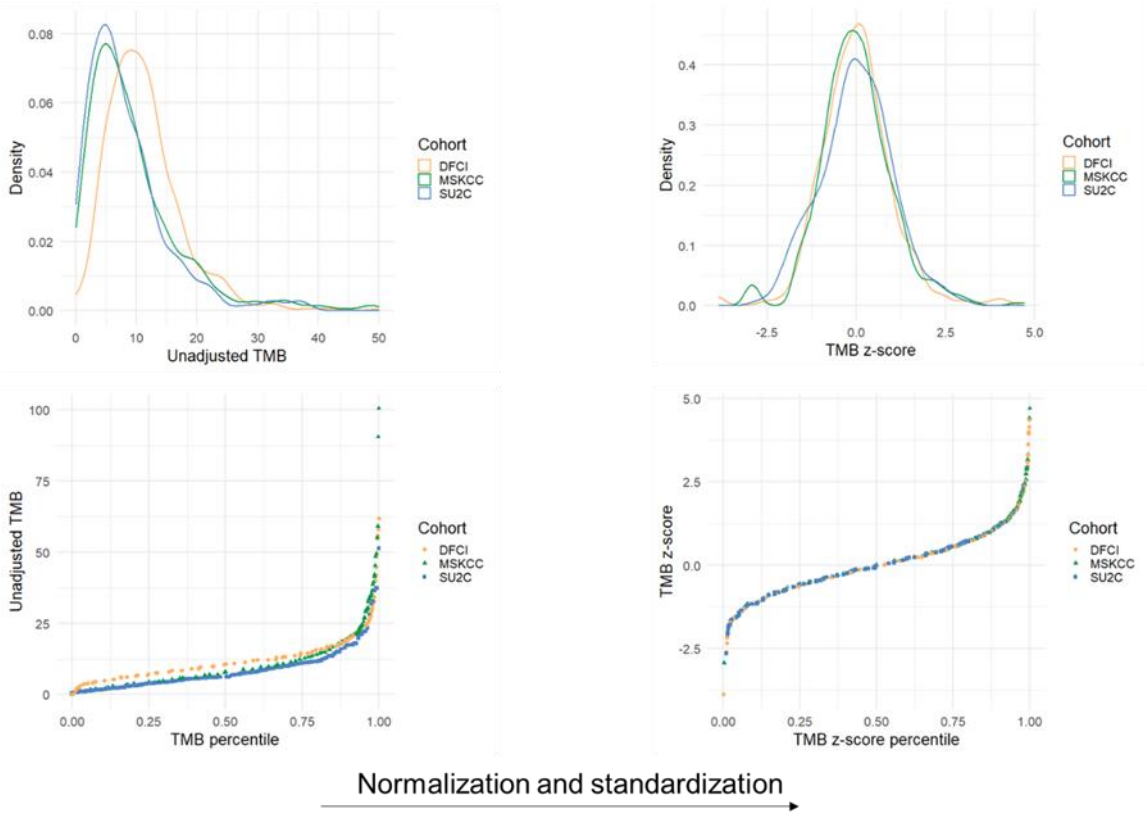

Figure 13. Normalization and standardization of TMB distributions bring the next-generation sequencing (MSK-IMPACT and

Next, we leveraged a robust statistical framework to identify an optima cut-off of TMB that was associated with improved ORR (**Figure 14**).

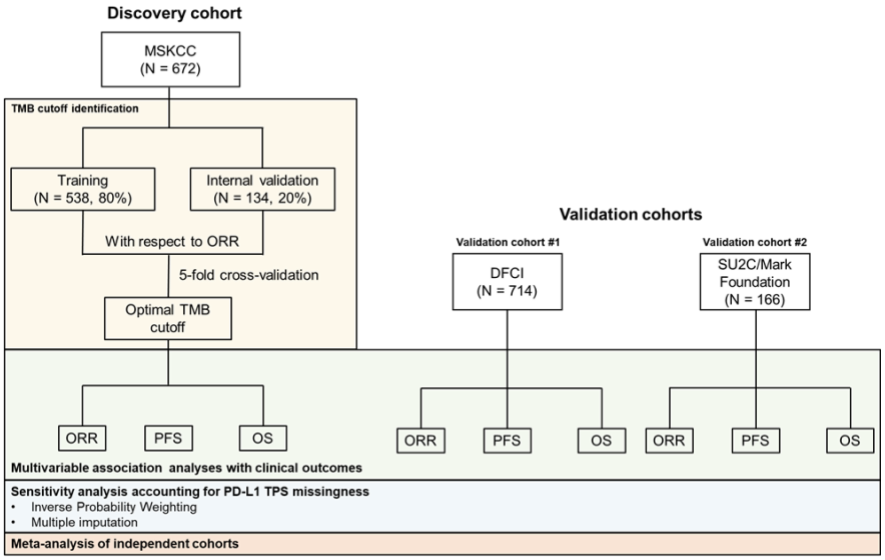

Figure 14. Statistical approach for the determination and validation of tumor mutational burden optimal cut-point in this study. MSKCC, Memorial Sloan Kettering Cancer Center; DFCI, Dana-Farber Cancer Institute; SU2C, Stand Up To Cancer/Mark Foundation; ORR, objective response rate; PFS, progression-free survival; OS, overall survival.DFCI OncoPanel) and WES cohort (SU2C/Mark Foundation) distributions into alignment. The left side shows the kernel density plot of unadjusted TMB values in each cohort, and the right side shows the transformed density plot of TMB z-scores that demonstrate high overlap.

We identified in each of the three independent cohorts that TMB at the 90th percentile was associated with improved ORR, PFS, and OS (not shown). We therefore applied this harmonized cut-off in the combined cohort and found that a very high TMB (at the 90th percentile of harmonized TMB) was associated with improved ORR, PFS, and OS (**Figure 15**). This association was also confirmed in multivariable analysis, after adjusting for confounders (PMID: 35708671)

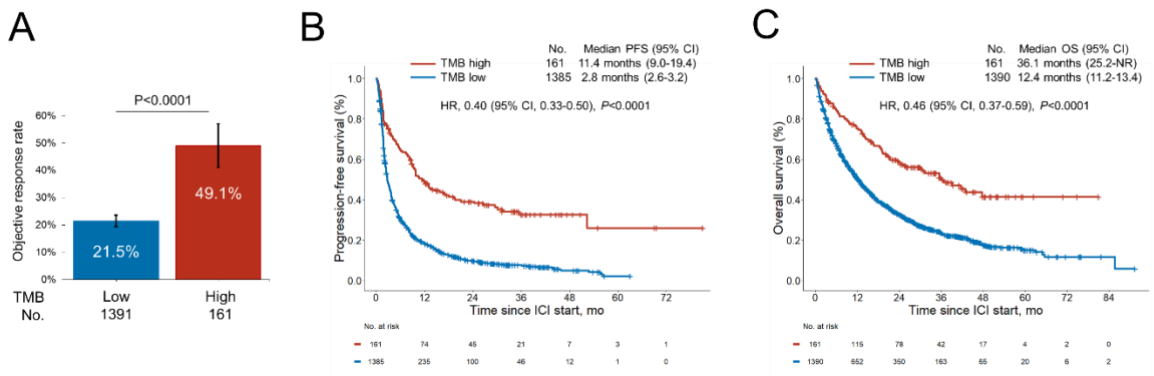

Figure 15. (A) Objective response rate, (B) progression-free survival, and (C) overall survival in patients with a high versus low harmonized TMB in the pooled cohort of 1552 NSCLCs treated with PD-(L)1 blockade from DFCI, MSKCC, and the SU2C/Mark Foundation dataset.

To explore mechanisms by which NSCLCs with high TMB are more responsive to ICI, we next performed multiplexed immunofluorescence (mIF) for CD8, Foxp3, PD-1, and PD-L1 on 428 NSCLC samples at DFCI. We found a significant association between higher TMB levels and increased CD8$^+$ T-cell counts intratumorally, at the tumor-stroma interface, and in total (**Figure 16A**); increased PD-1$^+$ cells at the tumor-stroma interface (**Figure 16B**); increased CD8$^+$ PD-1$^+$ T cells intratumorally, at the tumor-stroma interface, and in total (**Figure 16C**). No significant differences in intratumoral and total Foxp3$^+$ cells were identified in TMB high vs low cancers (**Figure 16D**).

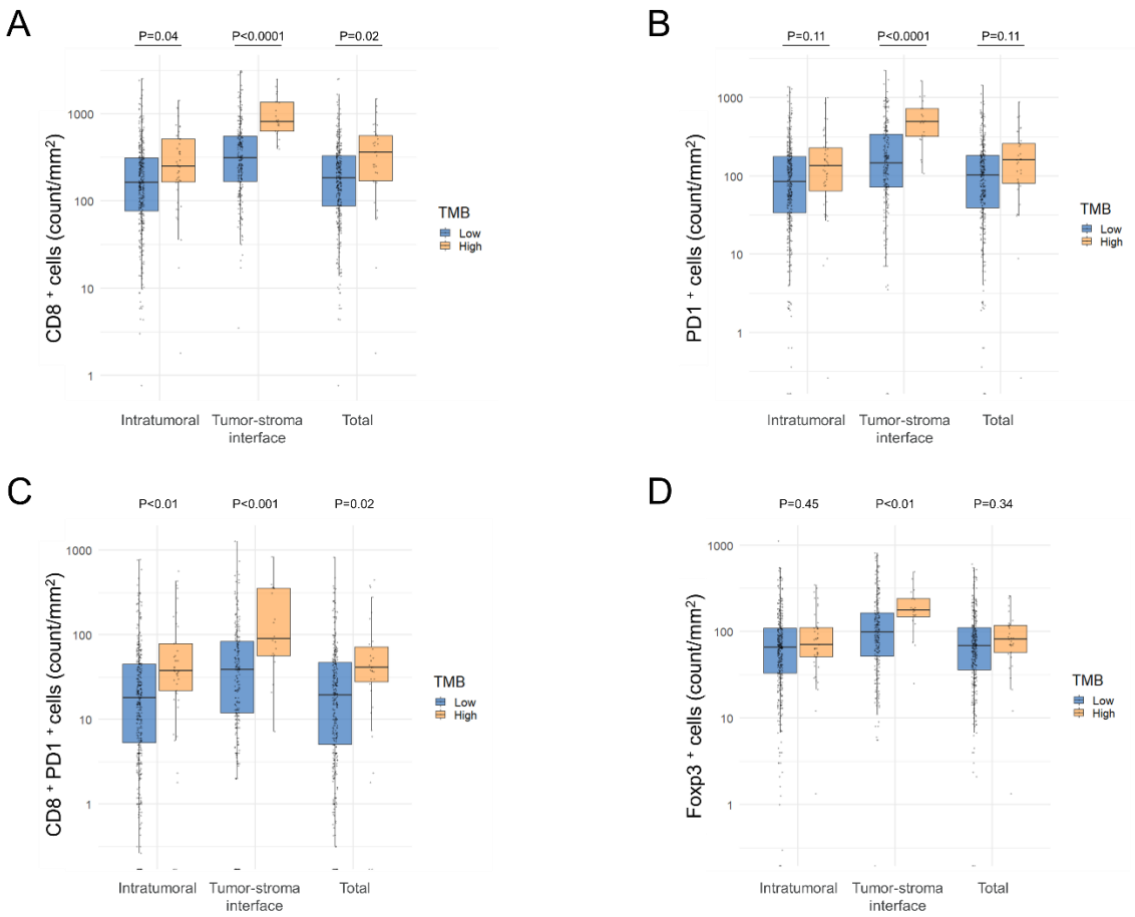

Figure 16. Multiplexed immunofluorescence (ImmunoProfile) showing intratumoral, tumor-stroma interface, and total (A) CD8+ cells, (B) PD1+ cells, (C) CD8+ PD1+ cells, and (D) Foxp3+ cells in TMB-low (N = 384) and TMB-high (N = 44) non-small cell lung cancers at DFCI.

Lastly, to investigate the differing effects of TMB and PD-L1 expression on clinical outcomes to ICI in the combined cohort, we examined the impact of the high vs low TMB threshold on ORR, PFS, and OS to ICI across the three clinically relevant PD-L1 expression subgroups of <1%, 1-49%, and ≥50%, as distinct PD-(L)1 based therapies have been approved based on these PD-L1 categories1-4. We identified that a high TMB (TMB Z-score >1.16 for each cohort) was associated with improved ORR and survival in each PD-L1 subset (**Table 2**), compared to a low TMB (TMB Z-score ≤1.16). Notably, patients with NSCLCs harboring both high TMB and PD-L1 expression ≥50% experienced an ORR of 57%, and had also the longest PFS (18.1 months) and OS (47.7 months) with ICI. In contrast, patients with TMB-low/PD-L1-negative NSCLC had the lowest ORR (~9%), and the shortest PFS (2.1 months) and OS (10.4 months). These data indicate that TMB can further stratify outcomes to

immunotherapy for patients within each clinically relevant PD-L1 expression group.

	PD-L1 TPS	TMB low	TMB high	P
ORR % (95%CI)	<1%	8.7% (2.6-10.3)	46.7% (28.3-65.7)	<0.0001
	1-49%	18.7% (6.9-18.1)	50.0% (19.4-57.6)	<0.001
	≥50%	38.1% (17.3-39.8)	56.5% (41.2-70.0)	0.017
PFS months (95%CI)	<1%	2.1 (2.0-2.4)	10.7 (8.2-24.4)	<0.0001
	1-49%	2.9 (2.5-3.6)	13.6 (8.6-NR)	<0.0001
	≥50%	5.2 (4.6-6.2)	18.1 (8.6-NR)	<0.001
OS months (95%CI)	<1%	10.4 (7.9-13.6)	23.9 (16.7-NR)	0.07
	1-49%	11.3 (9.6-14.7)	NR (21.2-NR)	<0.001
	≥50%	21.4 (17.5-25.9)	47.7 (35.4-NR)	0.02

Table 2. Objective response rate, progression-free, and overall survival to PD-(L)1 blockade in TMB-high and TMB-low NSCLC according to PD-L1 expression subgroups of <1%, 1-49%, and ≥50%

Discussion

In this thesis, we demonstrate that deleterious DDR mutations are common in advanced NSCLC, and the presence of these mutations is associated with improved clinical outcomes to treatment with PD-(L)1 inhibitors. We also demonstrate that this association is observed among patients with PD-L1 expression ≥50% treated with first-line pembrolizumab. Importantly, we found no difference in ORR and mPFS to first-line chemotherapy according to DDR mutation status. To our knowledge, this is the first study to demonstrate an independent association between deleterious DDR gene mutations and clinical benefit to PD-(L)1 inhibitor therapy in patients with advanced NSCLC. PD-L1 expression by immunohistochemistry is an imperfect predictive biomarker of PD-(L)1 inhibitor response, and the recent approval of pembrolizumab monotherapy for patients with PD-L1 expression ≥1% highlights an important and timely need for clinical tools that can distinguish patients who will benefit from PD-(L)1 inhibitor therapy alone versus those whose optimal treatment may

be the combination of a PD-(L)1 inhibitor plus doublet chemotherapy. The increased utilization of broad genomic profiling in the contemporary care of advanced NSCLC suggests that DDR mutation status may be a readily available genomic biomarker that could augment treatment decision making.

Along with PD-L1 expression, higher nonsynonymous tumor mutational burden is also associated with improved clinical outcomes to PD-1 blockade in patients with advanced NSCLC. In our analysis, TMB was associated with a longer PFS to immunotherapy but not a prolonged OS in multivariate analysis, which is consistent with recent data showing an improvement in PFS but not in OS in patients with high TMB treated with PD-(L)1 inhibitor therapy. Conversely, DDR mutation status was independently associated with improved PFS and OS in multivariable models, after controlling for TMB and PD-L1 expression. However, due to the collinearity between DDR mutations and TMB, the mutual independence of these two variables cannot be entirely demonstrated. While these findings appear to be a class effect, this study was not powered for subset analyses of individual DDR genes. In addition to the higher tumor mutational burden and the higher predicted neoantigenic load other non-neoantigen based mechanisms may contribute to explain this association. For instance, activation of the stimulator of interferon genes (STING) pathway as a result of cytosolic DNA fragment accumulation in the setting of DDR deficiency is an emerging potential mechanism that can foster potent antitumor immune response[13,30]. Therefore, the presence of DDR mutation should not be interpreted simply as a proxy for higher TMB and neoantigen load. Rather, these two measures should be integrated with the known predictive biomarkers, such as PD-L1 expression, to identify those patients that are more likely to respond to PD-(L)1 inhibitor therapy. However, additional studies will be needed on larger cohorts to determine whether individual DDR genes or DDR functional classes are different from others in term of TMB, PD-L1 expression and impact on clinical outcome to PD-(L)1 blockade in NSCLC

The identification and characterization of DDR mutation status in NSCLC may also have implications for novel combinatorial immuno-oncology strategies. Clinical trials combining PD-(L)1 inhibition with DNA repair targeted agents, including PARP and ATR inhibitors, in patients with DDR-mutant disease are ongoing. Combining PD-L1 expression levels with DDR mutation status might

enable improved biomarker selection to enhance the proportion of NSCLC patients who benefit from PD-(L)1 inhibitors.

Our findings also highlight that pathogenicity assessment is an important challenge relevant to the interpretation of DDR gene mutations identified by clinical genomic profiling. We classified loss-of-function mutations in DDR genes (including nonsense, frameshift, or splice site) as deleterious, and integrated several tools (COSMIC, ClinVar, and PolyPhen-2)²⁷²⁷²⁷²⁷²⁷²⁷ to determine the functional significance of missense mutations. When we analyzed the clinical outcomes to PD-(L)1 inhibitor therapy according to the strength of evidence for DDR mutation status, we found that clinical outcomes to immunotherapy were improved even for missense mutations that were not included in COSMIC and/or ClinVar but predicted to be deleterious through PolyPhen-2, compared to the DDR-negative cohort. Nonetheless, the number of missense mutations that were not included in COSMIC and/or ClinVar highlights that additional functional validation of DDR gene mutations in NSCLC is highly warranted. We acknowledge several limitations relevant to this aim: 1) this was a retrospective analysis of patients treated at a single academic cancer center; 2) a fraction of the mutations identified by this analysis have not had robust functional characterization; 3) COSMIC and ClinVar databases are dynamic, and the extent of functional validation underlying pathogenicity annotations in these databases is variable; 4) dedicated paired germline analysis was not performed; 5) OncoPanel is a targeted NGS assay that does not include coverage of all DDR genes.

In the second aim of this thesis, we demonstrated that mutations in *STK11* and *KEAP1* are frequent and define major subsets of *KRAS*^{MUT} LUADs, characterized by unique immune profiles and poor outcomes to ICI in two independent cohorts. Our results extend previous reports of LUAD with *STK11* mutations[18], and identify loss-of-function mutations in *KEAP1* as a frequent and independent driver of resistance to ICI in patients with advanced *KRAS*^{MUT} LUAD. To gain insights to potential mechanisms by which *STK11* and *KEAP1* loss exert deleterious effects on PD-(L)1 inhibition among *KRAS*^{MUT} but not *KRAS*^{WT} LUAD, we found that *KRAS*^{MUT}/*STK11*^{MUT} tumors had a significant downregulation of MHC class II compared to *KRAS*^{MUT}/*STK11*^{WT}, including,

HLA-DOA, *HLA-DRB5*, *HLA-DRB1*, and *HLA-DMB.* By contrast, *STK11* mutation was not associated with MHC class II pathway deregulation among *KRAS*^{WT} cases. The expression of MHC class II-restricted antigens by tumor cells is required for CD4+ T-cell activation to elicit anti-tumor immune responses, and MHC class II expression has been associated with improved PFS and OS in patients treated with ICI in multiple cancer types[31]. *KRAS*^{MUT}/*KEAP1*^{MUT} LUAD also showed a unique gene expression profile, characterized by significant downregulation of positive regulators of type I interferon and other inflammatory cytokines, including *TMEM173 (STING)*, *DDX58, TLR4,* and *TLR7*. While *STK11* loss has previously been reported to result in marked silencing of *STING* expression in *KRAS*-mutant LUAD[32], whether a similar mechanism could lead to impaired tumor immunogenicity in *KRAS*^{MUT}/*KEAP1*^{MUT} LUAD, is unknown, and deserves additional exploration.

These findings have implications for clinical trial interpretation and design as well as for treatment selection. Our study suggests that immunotherapy clinical trials should consider employing stratification measures to balance randomized groups for *STK11* and *KEAP1* co-mutation status and ensure that differences in outcomes are due to therapeutic interventions rather than variations in *STK11* and/or *KEAP1* mutation frequency, especially in *KRAS*-mutant NSCLC. Our findings could also inform on how to sequence or combine future treatment strategies in *KRAS*^{MUT} LUAD. Preliminary data have shown that direct KRAS inhibitors can produce responses in ~35-45% of patients with *KRAS* G12C-mutant NSCLC[33]. As more effective treatment options become available for *KRAS*^{MUT} LUAD, *STK11* and *KEAP1* mutation status might be a useful biomarker in determining the optimal treatment sequence, and KRAS G12C inhibitors might be better used prior to ICI in genomic subsets of NSCLC which are predicted not to respond to PD-1 based regimens. Whether KRAS inhibition could be used in combination with immunotherapy is an area of increasing interest. Preclinical data have shown that KRAS G12C inhibition reinvigorate the TME with CD8+ T cells, macrophages, and CD103+ cross-presenting dendritic cells[34], suggesting that direct KRAS inhibitors may synergize with ICI, particularly among genomically-defined LUADs that are not predicted to respond to immunotherapy alone. Phase I/II trials of sotorasib and adagrasib in combination with pembrolizumab in patients with advanced NSCLC with *KRAS*

G12C mutation are currently ongoing (NCT03600883, NCT04613596). Limitations of this aim include the retrospective design, and the lack of validation from published randomized clinical trials of ICI versus chemotherapy. In addition, PD-L1 expression was not available in 35.9% samples. However, to account for the potential selection bias resulting from PD-L1 TPS missingness we used an inverse probability weighting (IPW) in Cox regression analysis.

In the last aim, we identify that patients with high TMB levels (at the ~90th percentile) derive the greatest improvement in terms of response to treatment and survival. Importantly, we extended this observation to PD-L1 negative and positive cases, indicating that TMB can predict benefit from immunotherapies across all PD-L1 expression levels. Several of our findings may explain the mechanistic association between a high TMB and improved clinical outcomes, including higher proportions of tumor-infiltrating CD8+ PD1+ T cells, and increased PD-L1 tumor expression. Here, using the power of a large cohort of immunotherapy-treated patients, which was only possible through a harmonized analysis across different sequencing platforms, we found that high TMB levels correlated with improved ICI efficacy across different PD-L1 expression subgroups, which has important implications. For patients with advanced NSCLC and a PD-L1 TPS of ≥1% and ≥50%, two therapeutic regimens are approved for use: ICI alone or in combination with chemotherapy[1]. Because there are no prospective data comparing ICI alone to ICI plus chemotherapy, our results suggest that for patients with PD-L1 TPS of 1-49% or ≥50%, and very high TMB, ICI may be a reasonable treatment option as monotherapy, sparing the potential toxicities of adding chemotherapy. As high TMB is a robust and independent biomarker of response to ICI, our data also suggest that TMB should routinely be introduced as a stratification factor for immunotherapy clinical trials, to ensure that outcomes are impacted by treatment interventions, rather than imbalances in TMB distributions. Importantly, because genomic coverage can differ across sequencing platforms, these trials should utilize assays that provide at least ≥0.5 Mb, or optimally ≥0.8 Mb of coverage for sufficient and accurate TMB assessment. Limitations of this aim include the retrospective design and the lack of PD-L1 expression data for a fraction of patients.

References

1. Ricciuti B, Awad MM. What Is the Standard First-Line Treatment for Advanced Non–Small Cell Lung Cancer? *Cancer J*. 2020;26(6):485-495. doi:10.1097/PPO.0000000000000489
2. Socinski MA, Jotte RM, Cappuzzo F, et al. Atezolizumab for First-Line Treatment of Metastatic Nonsquamous NSCLC. *N Engl J Med*. 2018;378(24):2288-2301. doi:10.1056/NEJMoa1716948
3. Mok TSK, Wu YL, Kudaba I, et al. Pembrolizumab versus chemotherapy for previously untreated, PD-L1-expressing, locally advanced or metastatic non-small-cell lung cancer (KEYNOTE-042): a randomised, open-label, controlled, phase 3 trial. *Lancet*. 2019;393(10183):1819-1830. doi:10.1016/S0140-6736(18)32409-7
4. Reck M, Rodriguez-Abreu D, Robinson AG, et al. Pembrolizumab versus Chemotherapy for PD-L1-Positive Non-Small-Cell Lung Cancer. *N Engl J Med*. 2016;375(19):1823-1833. doi:10.1056/NEJMoa1606774
5. Gandhi L, Rodríguez-Abreu D, Gadgeel S, et al. Pembrolizumab plus chemotherapy in metastatic non-small-cell lung cancer. *N Engl J Med*. 2018;378(22):2078-2092. doi:10.1056/NEJMoa1801005
6. Pilié PG, Tang C, Mills GB, Yap TA. State-of-the-art strategies for targeting the DNA damage response in cancer. *Nat Rev Clin Oncol*. 2019;16(2):81-104. doi:10.1038/s41571-018-0114-z
7. Knijnenburg TA, Wang L, Zimmermann MT, et al. Genomic and Molecular Landscape of DNA Damage Repair Deficiency across The Cancer Genome Atlas. *Cell Rep*. 2018;23(1):239-254.e6. doi:10.1016/j.celrep.2018.03.076
8. Swisher EM, Lin KK, Oza AM, et al. Rucaparib in relapsed, platinum-sensitive high-grade ovarian carcinoma (ARIEL2 Part 1): an international, multicentre, open-label, phase 2 trial. *Lancet Oncol*. 2017;18(1):75-87. doi:10.1016/S1470-2045(16)30559-9
9. Golan T, Hammel P, Reni M, et al. Maintenance Olaparib for Germline BRCA -Mutated Metastatic Pancreatic Cancer. *N Engl J Med*. 2019;381(4):317-327. doi:10.1056/NEJMoa1903387
10. Litton JK, Rugo HS, Ettl J, et al. Talazoparib in Patients with Advanced Breast Cancer and a Germline BRCA Mutation. *N Engl J Med*.

2018;379(8):753-763. doi:10.1056/NEJMoa1802905

11. Mouw KW, Goldberg MS, Konstantinopoulos PA, D'Andrea AD. DNA damage and repair biomarkers of immunotherapy response. *Cancer Discov*. 2017;7(7):675-693. doi:10.1158/2159-8290.CD-17-0226
12. Teo MY, Seier K, Ostrovnaya I, et al. Alterations in DNA damage response and repair genes as potential marker of clinical benefit from PD-1/PD-L1 blockade in advanced urothelial cancers. *J Clin Oncol*. 2018;36(17):1685-1694. doi:10.1200/JCO.2017.75.7740
13. Sen T, Rodriguez BL, Chen L, et al. Targeting DNA damage response promotes antitumor immunity through STING-mediated T-cell activation in small cell lung cancer. *Cancer Discov*. 2019;9(5):646-661. doi:10.1158/2159-8290.CD-18-1020
14. Härtlova A, Erttmann SF, Raffi FAM, et al. DNA Damage Primes the Type I Interferon System via the Cytosolic DNA Sensor STING to Promote Anti-Microbial Innate Immunity. *Immunity*. 2015;42(2):332-343. doi:10.1016/j.immuni.2015.01.012
15. Teo MY, Bambury RM, Zabor EC, et al. DNA damage response and repair gene alterations are associated with improved survival in patients with platinum-treated advanced urothelial carcinoma. *Clin Cancer Res*. 2017;23(14):3610-3618. doi:10.1158/1078-0432.CCR-16-2520
16. Collisson EA, Campbell JD, Brooks AN, et al. Comprehensive molecular profiling of lung adenocarcinoma: The cancer genome atlas research network. *Nature*. 2014;511(7511):543-550. doi:10.1038/nature13385
17. Skoulidis F, Byers LA, Diao L, et al. Co-occurring genomic alterations define major subsets of KRAS-mutant lung adenocarcinoma with distinct biology, immune profiles, and therapeutic vulnerabilities. *Cancer Discov*. Published online 2015. doi:10.1158/2159-8290.CD-14-1236
18. Skoulidis F, Goldberg ME, Greenawalt DM, et al. STK11/LKB1 mutations and PD-1 inhibitor resistance in KRAS-mutant lung adenocarcinoma. *Cancer Discov*. Published online 2018. doi:10.1158/2159-8290.CD-18-0099
19. Romero R, Sayin VI, Davidson SM, et al. Keap1 loss promotes Kras-driven lung cancer and results in dependence on glutaminolysis. *Nat Med*. Published online 2017. doi:10.1038/nm.4407

20. Arbour KC, Jordan E, Kim HR, et al. Effects of co-occurring genomic alterations on outcomes in patients with KRAS-mutant non-small cell lung cancer. *Clin Cancer Res*. Published online 2018. doi:10.1158/1078-0432.CCR-17-1841
21. Best SA, De Souza DP, Kersbergen A, et al. Synergy between the KEAP1/NRF2 and PI3K Pathways Drives Non-Small-Cell Lung Cancer with an Altered Immune Microenvironment. *Cell Metab*. Published online 2018. doi:10.1016/j.cmet.2018.02.006
22. Galan-Cobo A, Sitthideatphaiboon P, Qu X, et al. LKB1 and KEAP1/NRF2 pathways cooperatively promote metabolic reprogramming with enhanced glutamine dependence inKRAS-mutant lung adenocarcinoma. *Cancer Res*. Published online 2019. doi:10.1158/0008-5472.CAN-18-3527
23. Strickler JH, Hanks BA, Khasraw M. Tumor Mutational Burden as a Predictor of Immunotherapy Response: Is More Always Better? *Clin Cancer Res*. 2021;27(5):1236-1241. doi:10.1158/1078-0432.CCR-20-3054
24. Hellmann MD, Ciuleanu TE, Pluzanski A, et al. Nivolumab plus ipilimumab in lung cancer with a high tumor mutational burden. *N Engl J Med*. 2018;378(22):2093-2104. doi:10.1056/NEJMoa1801946
25. Garcia EP, Minkovsky A, Jia Y, et al. Validation of OncoPanel: A Targeted Next-Generation Sequencing Assay for the Detection of Somatic Variants in Cancer. *Arch Pathol Lab Med*. 2017;141(6):751-758. doi:10.5858/arpa.2016-0527-OA
26. Cheng DT, Mitchell TN, Zehir A, et al. Memorial sloan kettering-integrated mutation profiling of actionable cancer targets (MSK-IMPACT): A hybridization capture-based next-generation sequencing clinical assay for solid tumor molecular oncology. *J Mol Diagnostics*. Published online 2015. doi:10.1016/j.jmoldx.2014.12.006
27. Adzhubei IA, Schmidt S, Peshkin L, et al. A method and server for predicting damaging missense mutations. *Nat Methods*. 2010;7(4):248-249. doi:10.1038/nmeth0410-248
28. Adzhubei IA, Schmidt S, Peshkin L, et al. PolyPhen-2 : prediction of functional effects of human nsSNPs. *Nat Methods*. Published online

2010. doi:10.1038/nmeth0410-248

29. Aran D, Hu Z, Butte AJ. xCell: Digitally portraying the tissue cellular heterogeneity landscape. *Genome Biol*. Published online 2017. doi:10.1186/s13059-017-1349-1
30. Parkes EE, Walker SM, Taggart LE, et al. Activation of STING-dependent innate immune signaling by s-phase-specific DNA damage in breast cancer. *J Natl Cancer Inst*. 2017;109(1). doi:10.1093/jnci/djw199
31. Alspach E, Lussier DM, Miceli AP, et al. MHC-II neoantigens shape tumour immunity and response to immunotherapy. *Nature*. 2019;574(7780):696-701. doi:10.1038/s41586-019-1671-8
32. Kitajima S, Ivanova E, Guo S, et al. Suppression of STING associated with lkb1 loss in KRAS-driven lung cancer. *Cancer Discov*. 2019;9(1):34-45. doi:10.1158/2159-8290.CD-18-0689
33. Désage AL, Léonce C, Swalduz A, Ortiz-Cuaran S. Targeting KRAS Mutant in Non-Small Cell Lung Cancer: Novel Insights Into Therapeutic Strategies. *Front Oncol*. 2022;12(February). doi:10.3389/fonc.2022.796832
34. Canon J, Rex K, Saiki AY, et al. The clinical KRAS(G12C) inhibitor AMG 510 drives anti-tumour immunity. *Nature*. Published online 2019. doi:10.1038/s41586-019-1694-1

Report on the research activity performed during the PhD program

Immune checkpoint blockade with programmed death 1 (PD-1) or programmed death ligand 1 (PD-L1) inhibitors is an integral component of standard treatment for most patients with advanced non-small cell lung cancer (NSCLC). However, the degree of benefit with PD-(L)1 inhibitor therapy is highly variable, and the identification of clinically-available biomarkers of response to these agents in NSCLC has been challenging. Although PD-L1 expression levels by immunohistochemistry broadly correlate to response to immunotherapy in NSCLC, patients with tumors across all PD-L1 expression levels (including negative expression) may derive prolonged clinical benefit from PD-(L)1 inhibitors, which highlights the need to identify novel biomarkers of immunotherapy efficacy and resistance. The aims of the research project include to determine the clinicopathologic and genomic determinants of response and resistance to immunotherapy in NSCLC. During the first year I aimed at determining the tumor-cells intrinsic mechanism of sensitivity and resistance to PD-(L)1 blockade in NSCLC harboring somatic mutations in DNA damage and repair (DDR) genes using comprehensive genomic profiling. By leveraging massive parallel tumor DNA sequencing, I found a significant association between the presence of DDR mutations and improved response rate and survival with PD-(L)1 blockade, as well as a significant association between DDR mutations and increased TMB. During my second year, I brought to completion another project in which I disentangled the impact of STK11 and KEAP1 mutation on clinical outcomes to PD-(L)1 blockade in NSCLC. In this second study I found that the detrimental impact of these two mutations on immunotherapy efficacy is limited to KRAS mutant lung cancers. Of note, I identified that these mutations also associate with a unique immunophenotype among KRAS mutant NSCLC but not among KRAS WT NSCLC. In the last year of this PhD program, I studied how to improve the use of tumor mutational burden for the prediction of immunotherapy efficacy in NSCLC. I identified that increasing levels of TMB are associated with benefit from PD-(L)1 blockade, with patients whose tumors have a TMB in the top decile deriving the greatest improvement in terms of response to treatment and survival. Importantly, this

study extended this observation to PD-L1 negative and positive cases, indicating that TMB can predict benefit from immunotherapies across all PD-L1 expression levels. In addition to these primary aims outlined in this thesis, I also contributed to other research efforts to understand mechanisms of primary and acquired resistance to PD-(L)1 blockade in NSCLC, as specified in each annual report.

Publications - XXV cycle PhD program

- **Ricciuti B**, Recondo G, Spurr LF, Li YY, Lamberti G, Venkatraman D, Umeton R, Cherniack AD, Nishino M, Sholl LM, Shapiro GI, Awad MM, Cheng ML. Impact of DNA Damage Response and Repair (DDR) Gene Mutations on Efficacy of PD-(L)1 Immune Checkpoint Inhibition in Non-Small Cell Lung Cancer. Clin Cancer Res. 2020 Aug 1;26(15):4135-4142.
- Lamberti G, Andrini E, Sisi M, Federico AD, **Ricciuti B**. Targeting DNA damage response and repair genes to enhance anticancer immunotherapy: rationale and clinical implication. Future Oncol. 2020 Aug;16(23):1751-1766
- Lamberti G, Spurr LF, Li Y, **Ricciuti B**, Recondo G, Umeton R, Nishino M, Sholl LM, Meyerson ML, Cherniack AD, Awad MM. Clinicopathological and genomic correlates of programmed cell death ligand 1 (PD-L1) expression in nonsquamous non-small-cell lung cancer. Ann Oncol. 2020 Apr 27;S0923-7534(20)36078-6
- Alessi JV, **Ricciuti B**, Jiménez-Aguilar E, Hong F, Wei Z, Nishino M, Plodkowski AJ, Sawan P, Luo J, Rizvi H, Carter BW, Heymach JV, Altan M, Hellmann M, Awad MM. Outcomes to first-line pembrolizumab in patients with PD-L1-high (≥50%) non-small cell lung cancer and a poor performance status. J Immunother Cancer. 2020 Aug;8(2):e001007
- Gainor JF, Rizvi H, Jimenez Aguilar E, Skoulidis F, Yeap BY, Naidoo J, Khosrowjerdi S, Mooradian M, Lydon C, Illei P, Zhang J, Peterson R, **Ricciuti B**, Nishino M, Zhang J, Roth JA, Grishman J, Anderson D, Little BP, Carter BW, Arbour K, Sauter JL, Mino-Kenudson M,

Heymach JV, Digumarthy S, Shaw AT, Awad MM, Hellmann MD. Clinical activity of programmed cell death 1 (PD-1) blockade in never, light, and heavy smokers with non-small-cell lung cancer and PD-L1 expression ≥50. Ann Oncol. 2020 Mar;31(3):404-411

- Wang X, **Ricciuti B**, Alessi JV, Nguyen T, Awad MM, Lin X, Johnson BE, Christiani DC. Smoking History as a Potential Predictor of Immune Checkpoint Inhibitor Efficacy in Metastatic Non-Small Cell Lung Cancer. J Natl Cancer Inst. 2021 Jun 11
- Wang X, **Ricciuti B**, Nguyen T, Li X, Rabin MS, Awad MM, Lin X, Johnson BE, Christiani DC. Association between Smoking History and Tumor Mutation Burden in Advanced Non-Small Cell Lung Cancer. Cancer Res. 2021 May 1;81(9):2566-2573
- **Ricciuti B**, Jones G, Severgnini M, Alessi JV, Recondo G, Lawrence M, Forshew T, Lydon C, Nishino M, Cheng M, Awad M. Early plasma circulating tumor DNA (ctDNA) changes predict response to first-line pembrolizumab-based therapy in non-small cell lung cancer (NSCLC) J Immunother Cancer. 2021 Mar;9(3):e001504.
- **Ricciuti B**, Alessi JV, Elkrief A, Wang X, Cortellini A, Li YY, Vaz VR, Gupta H, Pecci F, Barrichello A, Lamberti G, Nguyen T, Lindsay J, Sharma B, Felt K, Rodig SJ, Nishino M, Sholl LM, Barbie DA, Negrao MV, Zhang J, Cherniack AD, Heymach JV, Meyerson M, Ambrogio C, Jänne PA, Arbour KC, Pinato DJ, Skoulidis F, Schoenfeld AJ, Awad MM, Luo J. Ann Oncol. 2022 Jul 22:S0923-7534(22)01856-7.
- Cortellini A, **Ricciuti B**, Borghaei H, Naqash AR, D'Alessio A, Fulgenzi CAM, Addeo A, Banna GL, Pinato DJ. Differential prognostic effect of systemic inflammation in patients with non-small cell lung cancer treated with immunotherapy or chemotherapy: A post hoc analysis of the phase 3 OAK trial. Cancer. 2022 Aug 15;128(16):3067-3079.
- **Ricciuti B**, Wang X, Alessi JV, Rizvi H, Mahadevan NR, Li YY, Polio A, Lindsay J, Umeton R, Sinha R, Vokes NI, Recondo G, Lamberti G, Lawrence M, Vaz VR, Leonardi GC, Plodkowski AJ, Gupta H, Cherniack AD, Tolstorukov MY, Sharma B, Felt KD, Gainor JF, Ravi A, Getz G, Schalper KA, Henick B, Forde P, Anagnostou V, Jänne PA,

Van Allen EM, Nishino M, Sholl LM, Christiani DC, Lin X, Rodig SJ, Hellmann MD, Awad MM. Association of High Tumor Mutation Burden in Non-Small Cell Lung Cancers With Increased Immune Infiltration and Improved Clinical Outcomes of PD-L1 Blockade Across PD-L1 Expression Levels. JAMA Oncol. 2022 Aug 1;8(8):1160-1168

- Cortellini A, **Ricciuti B**, Vaz VR, Soldato D, Alessi JV, Dall'Olio FG, Banna GL, Muthuramalingam S, Chan S, Majem M, Piedra A, Lamberti G, Andrini E, Addeo A, Friedlaender A, Facchinetti F, Gorría T, Mezquita L, Hoton D, Valerie L, Nana FA, Artingstall J, Comins C, Di Maio M, Caglio A, Cave J, McKenzie H, Newsom-Davis T, Evans JS, Tiseo M, D'Alessio A, Fulgenzi CAM, Besse B, Awad MM, Pinato DJ. Prognostic effect of body mass index in patients with advanced NSCLC treated with chemoimmunotherapy combinations J Immunother Cancer. 2022 Feb;10(2):e004374
- Cheng ML, Milan MSD, Tamen RM, Bertram AA, Michael KS, **Ricciuti B**, Kehl KL, Awad MM, Sholl LM, Paweletz CP, Jänne PA. Plasma cfDNA Genotyping in Hospitalized Patients With Suspected Metastatic NSCLC JCO Precis Oncol. 2021 Nov;5:726-732
- **Ricciuti B**, Arbour KC, Lin JJ, Vajdi A, Vokes N, Hong L, Zhang J, Tolstorukov MY, Li YY, Spurr LF, Cherniack AD, Recondo G, Lamberti G, Wang X, Venkatraman D, Alessi JV, Vaz VR, Rizvi H, Egger J, Plodkowski AJ, Khosrowjerdi S, Digumarthy S, Park H, Vaz N, Nishino M, Sholl LM, Barbie D, Altan M, Heymach JV, Skoulidis F, Gainor JF, Hellmann MD, Awad MM. Diminished Efficacy of Programmed Death-(Ligand)1 Inhibition in STK11- and KEAP1-Mutant Lung Adenocarcinoma Is Affected by KRAS Mutation Status J Thorac Oncol. 2022 Mar;17(3):399-410
- Alessi JV, **Ricciuti B**, Alden SL, Bertram AA, Lin JJ, Sakhi M, Nishino M, Vaz VR, Lindsay J, Turner MM, Pfaff K, Sharma B, Felt KD, Rodig SJ, Gainor JF, Awad MM. Low peripheral blood derived neutrophil-to-lymphocyte ratio (dNLR) is associated with increased tumor T-cell infiltration and favorable outcomes to first-line pembrolizumab in non-small cell lung cancer J Immunother Cancer. 2021 Nov;9(11):e003536.